Development of a pharmacokinetic imaging system for astatine-211 in the whole body of mice

A. Yagishita,[*1] S. Takeda,[*1] M. Katsuragawa,[*1] and T. Takahashi[*1]

Recently, targeted α therapy (TAT) has gained much attention. α-particle emitting pharmaceuticals can cause severe damage to all types of cells owing to the potency of α-particles. Therefore, optimizing carrier agents for α-emitters to accumulate in cancer is crucial. This can be achieved by minimizing accumulation in normal tissues and reducing adverse effects. Therefore, imaging of pharmacokinetics in mice can help development of agents for TAT. However, pharmacokinetic in vivo imaging of α-particle emitting agents is challenging due to the low administration dose. Increasing spatial resolution decreases sensitivity. Therefore, to achieve higher sensitivity, it is crucial to estimate the minimum spatial resolution required for detecting small organs in mice, such as the thyroid, and to adjust the collimator accordingly by thinning the collimator septa and reducing the thickness of the collimator. Additionally, obtaining accurate dose is crucial. To achieve this, noise signals such as scattering components and fluorescent X-rays should be removed as much as possible. For this purpose, a detector with higher energy resolution is desired.

To address these problems, we developed a imaging system optimized for pharmacokinetic imaging of astatine (At)-211-labeled agents (CdTe XG-Cam). This system has a 3D-printed tungsten collimator and a cadmium-telluride (CdTe) semiconductor detector (0.75 mm-thick). The field of view (FOV) covers half of a mouse's body.[1)] After verification of its performance and feasibility for practical use, we developed an improved version of the system that has higher sensitivity owing to further optimization of a collimator.[2)] We conducted experiments using At-211 produced in the ^{209}Bi$(\alpha, 2n)^{211}$At reaction at the RIKEN AVF cyclotron. An image of At-211-loaded Derenzo phantom generated by using X-rays from At-211 (Po-211 K_α line) indicates that the spatial resolution is approximately 1.6 mm (Fig. 1a). Spectra obtained in Derenzo phantom imaging revealed that X-rays from At-211 and the fluorescent X-rays from tungsten were distinguishable owing to the high energy resolution of a CdTe detector (Fig. 1b). In vivo imaging of cancer-bearing mouse was performed in the therapeutic experiments using K1 and NIS-expressing K1 (K1-NIS) cancer cells. NIS is responsible for incorporating At into cells, and therefore, NIS-expressing cancers can be treated with At-211-NaAt. Accumulation of At-211-NaAt in the K1-NIS tumor could be clearly imaged compared to the K1 tumor using CdTe XG-Cam.

As mentioned above, our previous study demonstrated quantitative in vivo imaging of At-211 was feasible and useful. However, CdTe XG-Cam had room for improvement in FOV and sensitivity. To address the challenges, a new imager that has FOV covering a whole mouse body was developed (XCam-CdTe, Fig. 2a). Using 2 mm-thick CdTe detector, its sensitivity was elevated. In vivo imaging of a cancer-bearing mouse with a NIS-expressing and a non-expressing tumor revealed At-211 distribution in the whole mouse body in an acquisition time of 10 min (Fig. 2b) thereby indicating that, XCam-CdTe is useful for drug development of At-211-labeled agents.

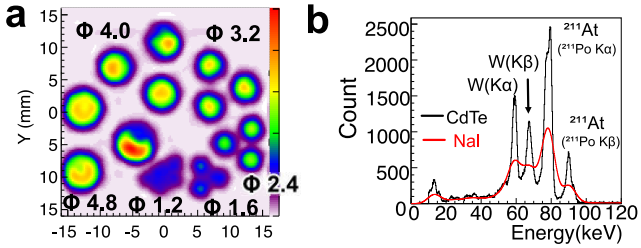

Fig. 1. Derenzo phantom imaging using At-211. **(a)** An image of the phantom using X-rays from At-211 (Po-211 K$_\alpha$ line). Φ indicates bore diameter (mm). **(b)** The X-rays from At-211 obtained by a CdTe detector are clearly distinguishable from the fluorescent X-rays of tungsten (black line) compared to those obtained by simulation using the representative energy resolution of NaI scintillator (red line).

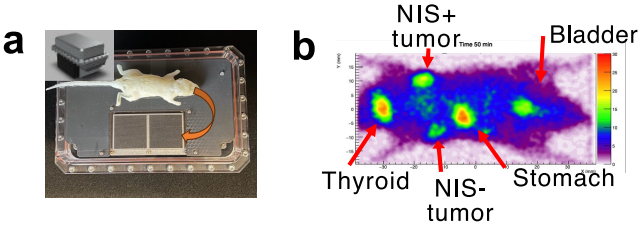

Fig. 2. **(a)** Top view of XCam-CdTe. Incet: the exterior of XCam-CdTe. **(b)** In vivo imaging of cancer-bearing mouse administerd 1.0 MBq of At-211 with a 10-minute acquition time shows accumulation of At-211 in NIS-positive tumor. Note that At-211 also accumultes in NIS-expressing normal tissues (*i.e.*, thyroid and stomach).

References
1) H. Fujii *et al.*, Radioisotopes **71**, 141 (2022).
2) A. Yagishita *et al.*, Bioengineering **11**, 25 (2023).

*1 Kavli IPMU, University of Tokyo

DOI:10.34448/RIKEN.APR.57-007